Design and Modelling of the Powertrain of a Hybrid Fuel Cell Electric Vehicle

21PFL-0123

Design and Modelling of the Powertrain of a Hybrid Fuel Cell Electric Vehicle

Author, co-author (Do NOT enter this information. It will be pulled from participant tab in MyTechZone)
Affiliation (Do NOT enter this information. It will be pulled from participant tab in MyTechZone)

Abstract

This paper presents a fuel cell electric vehicle (FCEV) powertrain development and optimization, aiming to minimize hydrogen consumption. The vehicle is a prototype that run at the Shell Eco-marathon race and its powertrain is composed by a PEM fuel cell, supercapacitors and a DC electric motor. The supercapacitors serve as an energy buffer to satisfy the load peaks requested by the electric motor, allowing a smoother (and closer to a stationary application) working condition for the fuel cell. Thus, the fuel cell can achieve higher efficiency rates and the fuel consumption is minimized.

Several models of the powertrain were developed using MATLAB-Simulink and then experimentally validated in laboratory and on the track. The proposed models allow to evaluate two main arrangements between fuel cell and supercapacitors: 1) through a DC/DC converter that sets the FC current to a desired value; 2) using a direct parallel connection between fuel cell and supercapacitors.

The results obtained with the direct parallel connection (with the appropriate sizing of the overall capacity) have highlighted a significant efficiency advantage, while the DC/DC converter insertion enables an improved control of the fuel cell current and requires a smaller capacitance.

Furthermore, a sizing methodology for the supercapacitors capacitance is proposed for both layouts: with the DC/DC converter it mainly depends on the energy range provided by supercapacitors to the electric motor, while in the direct parallel connection the supercapacitors sizing is outlined by concurrently evaluating the circuit's predicted hydrogen consumption and granting the most suitable conditions to increase the fuel cell performance.

Finally, the results obtained from the model were validated by comparing them with experimental data obtained in the laboratory and on the track.

Introduction

According to data from the International Energy Agency, the transport sector accounts for 29% of total energy consumption and 24.6 % of total CO_2 emissions [1,2]. The global transport system has doubled CO_2 emissions in the last 30 years so this requires a strong cut in emissions in order to fight the irreversible climate change [3]. For these

reasons, in order to reduce the impact of the transport sector on the environment, it is necessary to use alternative fuels.

Therefore, in order to decarbonise the transport system through a long-term strategy, it is necessary both to reduce vehicle total mass with lightweight techniques [4,5] and improve aerodynamic drag [6–8] and use low-carbon fuels with highly efficient powertrain [9–13]. So as regards the ICEs the choice falls on biofuels and as regards electric vehicles there are various options.

ICE: the main biofuels used within the ICEs are bio-ethanol and bio-diesel which lead to a reduction in CO_2 emissions, greater independence from oil-producing countries and in many cases also a more rational use of arable land [14];
MHEV: A mild hybrid system refers to a system consisting of a reversible electric machine that recovers energy under braking and in certain driving phases supplies the thermal engine with additional power.
HEV: A hybrid system has a larger battery compared to a MHEV that allows you to travel short electric distances with limitations regarding power and speed [13].
PHEV: Compared to HEV, this system has a larger battery that allows greater autonomy and the possibility of recharging through the power socket and regenerative braking.
BEV: it has the absence of an internal combustion engine and therefore always has zero emissions in each work cycle with autonomy varying according to the capacity of the battery pack.
FCEV: It incorporate a fuel cell that powers an electric motor, sometimes in combination with battery and supercapacitors (HFCEV).

The FCEVs therefore have intermediate characteristics compared to the BEV and ICE vehicles, and therefore represent one of the most interesting proposals for future mobility for a series of reasons:

- The FCEVs turn out to be one of the two truly zero-emission[1] alternatives and have an efficiency significantly higher than ICEs vehicles (50 % vs 25 %);
- The FCEVs can guarantee the comfort typical of an electric drive and the advantages in terms of autonomy and charging times typical of an ICE vehicle.
- FCEV vehicles have an energy storage (tank containing pressurized hydrogen at 700 bar) having a higher energy density than ion-batteries (1.55 kWh/L vs 0.4 kWh/L), thus making the FCEVs suitable for powering road vehicles in a wide range from small vehicles to buses or trucks.
- Hydrogen can be produced from any primary source of energy and potentially with zero emissions, in particular it can be noted that hydrogen can be produced mainly through the use of electricity produced from renewable sources, using an electrolyser that converts the water in hydrogen using electricity, or using fossil sources mainly through the “steam reforming process” and using CCS to sequester the flow of carbon dioxide produced by the production process [3].

There are different types of Fuel cells which are mainly characterized based on the type of electrolyte, temperature of use, type of fuel that can be used. The most used in the automotive field is the proton exchange membrane (PEM) type characterized by a solid polymer electrolyte, these cells run at quite low temperatures, so the problem of slow reaction rates is addressed by using sophisticated catalysts and electrodes [15,16].

The slow dynamics and the sensitivity of the cell components to power peaks imply that the fuel cell should operate in a steady-state and fast transient should be avoided in order to maximize the efficiency, minimize mechanical stresses and therefore increase the lifetime. In all applications where the load has strong variations, it is necessary to couple the fuel cell to another power source such as supercapacitors capable of managing the instantaneous power flow required by the load, thus maximizing the performance of the powertrain.

According to Atwood et al. [17] the hybridization of a FCEV can improve energy efficiency by as much as 50% and some other papers show even the purchase price of Fuel cell can be reduced by increasing the ratio between the auxiliary source’s maximum power to the powertrain total power - also known as degree of hybridization (DOH) - and thus through hybridization it is possible to reduce the powertrain capital cost and the operating cost by increasing efficiency [18–20].

1 It means zero emissions from the point of view of emissions directly attributable to the vehicle, therefore indirect emissions are not considered in this discussion.

Three different configurations of hybrid power-source are mainly used:

The two-converter structure includes the use of a converter and a control loop for each power source in particular as shown in Figure 1 a DC-DC converter connects the FC to the DC bus and a current reversible DC-DC converter connects the supercapacitors to the DC bus [21]. This system has advantages in terms of control flexibility but disadvantages in terms of overall system efficiency as the use of two converters implies additional losses.

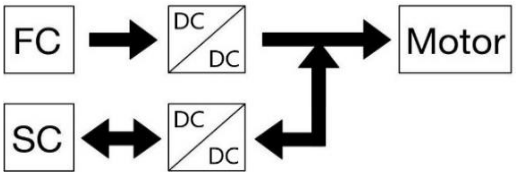

Figure 1. The two-converter configuration

The one-converter structure includes the use of a single converter that regulates the power flows supplied by the single power sources (Figure 2), in particular it is possible to guarantee good control and reduce the losses in terms of efficiency highlighted in the previous solution.

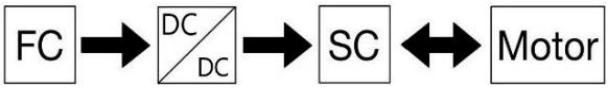

Figure 2. Scheme of the “one converter” structure

The direct parallel structure consists in connecting the FC directly to the supercapacitors (Figure 3) in order to reduce the losses associated to the use of DC/DC converter, but in order to be able to regulate the power and therefore the current delivered by the FC it is necessary to increase the capacitance of the supercapacitors [22,23].

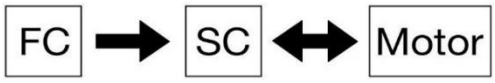

Figure 3. Scheme of the “direct parallel” structure

As case study have been used the IDRAkronos FCEV (Figure 4) developed by the Team H2Polito of the Politecnico di Torino.

Figure 4. IDRAkronos FCEV by H2PolitO

IDRAkronos is a hydrogen prototype built for the Shell Eco Marathon, and therefore aiming to minimize the consumption of hydrogen. It has the characteristics shown in Table 1:

Table 1. IDRAkronos vehicle data

Vehicle mass	39kg
Driver mass	50kg
Front wheels	2
Rear wheels	1
Dimensions	3341 mm; 807 mm; 561 mm
Type of Fuel cell	PEM Open cathode
Fuel cell cooling	Fan
Type of Electric	DC-Brushed (MAXON RE50
Transmission	Direct Meshing
Transmission	19
Supercapacitors	EDLCs
Max. speed	40 km/h

The paper was developed from the work conducted by the Team in order to optimize the vehicle. The Fuel Fell Division of the Team studies the powertrain of the vehicle in order to make the prototype more and more efficient year by year and to make it competitive in the Shell Eco Marathon. The first type of powertrain that was developed was made up of the fuel cell without any energy storage system. Subsequently, observing the behavior of the FC, it has been thought about strategies to ensure that the FC operates at maximum efficiency and it have started implementing on hybrid configurations. Two hybrid configurations have been developed: the one with a converter and the direct parallel.

Rajashekara et al. [24] explains qualitatively the different hybrid powertrain configurations, showing also the different fuel cells, converters and motors that can be used. This paper however gives a more quantitative description of the powertrain. For both the configurations have been developed a sizing method for the supercapacitors and a detailed powertrain model. Usually the approach used for the sizing of supercapacitors is to consider the required storage capacity, the maximum voltage and the current dynamics of the FC [25]. In this paper a model will be presented that takes into account in the process of sizing and optimizing of supercapacitors, also the influence on the thermal behavior of the FC and parameters related to the dynamic behavior of the vehicle that affect the powertrain energy demand.

Methods

Theoretical and analytical analysis

The fuel cell, as a source of electrical energy, has a typical current-voltage characteristic that is called polarization curve (Figure 5 - left). As the current increases, the voltage decreases due to internal losses of various kinds that produce heat. The losses can be associated to three different charge/mass transport phenomena:

- Charge transfer related to kinetic behavior of electro-chemical reaction;
- Charge conduction related to ion conduction in the electrolyte and electrons in the electrodes and external circuits;
- The transport related to molecules diffusion through the electrodes' pores;

Theoretically, considering the thermodynamic efficiency, the open voltage of a PEMFC cell at standard conditions is 1.23V. The electrical efficiency can be calculated by dividing the voltage of a single cell by this

value, in this way it can be understood that at high currents the efficiency of the fuel cell is reduced (Figure 5 - right).

When a fuel cell in a vehicle directly powers the electric motor (without energy storage systems) it must follow the power profile required by the motor, which typically has strong current fluctuations. In this type of configuration, the fuel cell works at a variable efficiency depending on the instantaneously power required which reaching high values leads to a reduced efficiency as shown in Figure 5. The direct consequence is that more hydrogen is consumed than if the fuel cell was working in steady state conditions at an average power value.

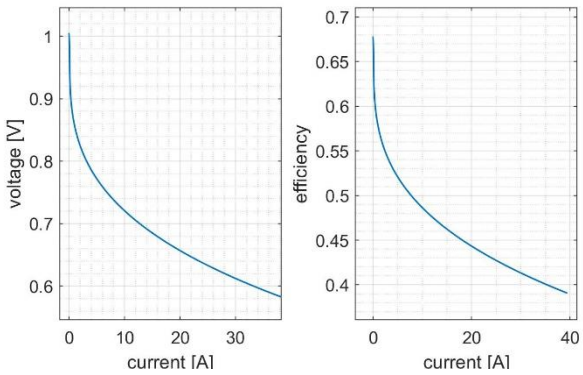

Figure 5. Polarization (left) and efficiency (right) curves

Furthermore, there are two indirect consequences that imply an additional hydrogen consumption: heat production and dehydration of the membrane.

The profile of heat produced, being a function of the current as shown in Eq. (1) presents generation peaks which therefore leads to an increase in the consumption of the auxiliaries used for cooling, in particular in the case of IDRAkronos it is necessary to use fans to high rates of PWM in order to avoid reaching excessively high temperatures and in this way the cathode humidity is reduced.

$$\left|\dot{Q}_{\text{th}}\right| = \left(\frac{-\Delta\bar{h}_{react}}{z * F} - \frac{V_{FC}}{nc}\right) * I \qquad (1)$$

Where Q_{th} is the heat produced, Δh_{react} the molar enthalpy of the reaction, z is the charge number of hydrogen, F the Faraday constant, V_{FC} represents the fuel cell voltage, nc is the number of cells and I the fuel cell current.

High currents, at the same time result in a high production of cathode water. An uneven humidification of the membrane implies a high resistance to the passage of protons and consequently the losses would increase [26,27]. For that, it is possible to implement two techniques:

- Short circuit the fuel cell for a short time[2] to instantly increase the production of water being the production of water directly proportional to the current.

2 Usually this technique is used for a time interval of the order of 100-200 ms according to the needs of the fuel cell in terms of benefits in the production of water and the consumption of hydrogen associated with this technique.

- Purge at the fuel cell anode in order to redistribute water evenly on the membrane, whereas this technique also involves a loss of hydrogen (the losses can be compensated with recirculation systems, if their consumption is worth).

To optimize the consumption of hydrogen it is necessary to use an energy storage system that allows the motor to work properly and at the same time to run the fuel cell as steadily as possible. The fuel cell then works at a continuous reduced power, equal to the average power required by the motor, meaning a higher efficiency than in non-hybrid configuration. Losses are reduced and since the heat produced is lower, the operating costs related to the auxiliaries used for cooling are reduced, in the case of IDRAkronos the use of the fans, short circuits and purges is also reduced.

A hybrid system of this type, considering an ideal storage system, is more efficient than a fuel cell system alone. However, in order to achieve this, it is necessary to use a real energy storage system that has losses as a result. It could be used batteries; they can accumulate large amounts of energy per unit of weight, but they are not ideal for application in high performance vehicles; the optimal choice falls in the use of supercapacitors. They are the main element of the energy storage system, they have a very high efficiency of the charge-discharge process, higher than batteries. To maintain a low weight, active carbon supercapacitors (EDLC), or rather lithium-ion supercapacitors (LIC), are used.

To build the electric energy storage system for IDRAkrons prototype, the one converter and direct parallel connection configurations presented in the introduction were designed and developed, while the configuration with two converters was not developed as it entailed too high losses compared to the benefits obtained in terms of control.

In one converter architecture (Figure 2) the fuel cell current is set at a constant value. The voltage of the supercapacitors in this way can be different from that of the fuel cell and can vary over a wide range without affecting the current of the fuel cell. This configuration guarantees a good control and stability, but it leads to losses in the converter: the efficiency of IDRAkronos' converter is 93%.

Direct parallel configuration – or "passive charging" (Figure 3) uses the supercapacitors directly in parallel to the fuel cell, the charging current and therefore the FC current depends on the supercapacitors voltage. The voltage of the supercapacitors establishes the current supplied by the fuel cell, since it's desired to keep the current supplied by the fuel cell at a value as constant as possible the supercapacitors capacitance must be chosen properly. In order to identify the optimal capacitance it is necessary to find a tradeoff between a sufficiently high value of capacitance that allows the electrical efficiency of the powertrain to be high, and a low weight in order to avoid increasing the losses due to the vehicle dynamics.

Model development

To design the IDRAkronos vehicle powertrain and evaluate the performance, a model-based approach was chosen. In the recent years, this approach has become an industry standard for conducting tests and validations [28]. Developing a model before even the final product is manufactured has great advantages in terms of time and cost [28–30]. The challenge is to develop a model that is as close to reality as possible while often having a limited amount of available data. When a model is being developed it is looked for at the same time to best describe all the components without complicating it excessively, for such reason it becomes necessary to describe some components more detailed while simplifying others depending on the goals of the study [30].

In order to develop the IDRAkronos vehicle powertrain a series of models have been developed using MATLAB/Simulink. The models were developed in a continuous field, using the "ode45-Runge-Kutta" variable step integration method. For the choice of the maximum time step usable by the integration method, a time convergence was carried out in order to evaluate the optimal value in terms of solution accuracy and computational cost.

Time Convergence

To perform a time convergence, it is necessary to identify the significant output of the model under examination, a range of step times within which to carry out the simulations and the reference value against to which to evaluate the relative error. Several different values were tested to assess their quality. Since an exact solution is not available, the solution obtained with a low step time (0.0005 s) is used as a reference.

The result in terms of hydrogen consumed during the race run was used as a significant output of the model in question. The norm operator is used to evaluate the instant by instant distance between the value of the quantity under examination, for a determined step time, against to the quantity under examination evaluated for the reference step time. It is evaluated the Euclidian norm which is defined as:

$$||v|| = \sqrt{\sum_{k=1}^{N} |v_k|^2} \qquad (2)$$

Where v is the vector and N the number of elements. The result was represented in Figure 6 in log-log scale. For this study, the relative error value of 10^{-3} was considered as an objective.

This target value is reached with a step time equal to about 0.02 s, while convergence is reached for a value equal to 0.01 s. Analysing the graph in Figure 6 it is possible notice that for step time values lower than 0.01 s no improvement is obtained in terms of convergence of the result and therefore from the point of view of the accuracy of the solution the ideal step time is 0.01 s.

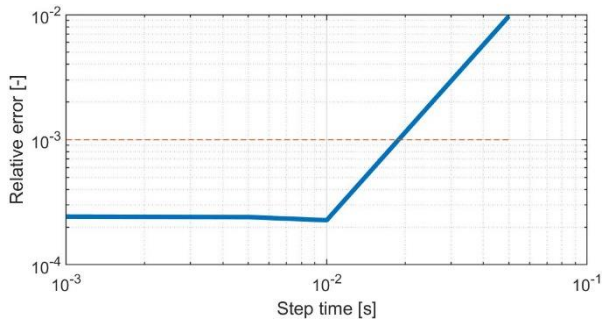

Figure 6. Time convergence study

Computational time analysis

In order to be able to do a cost-benefit analysis, it is necessary to evaluate the computational time trend as a function of the step time used (Figure 7). It is worth mentioning that the computational time depends on the type of processor used and the characteristics of the machine used, what is interesting is to evaluate the trend from a qualitative point of view.

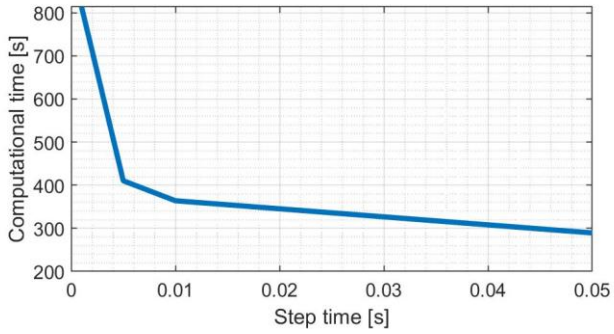

Figure 7. Computational time study

It can be noted that for step time values between 0.05 s and 0.005 s the computational time results to have a linear trend with a low slope while for values lower than 0.005 s the trend becomes exponential and therefore it is disadvantageous to further reduce the step time. Therefore, using a multi-objective analysis it is possible to obtain the best for our application as a time step of 0.01 s.

Powertrain model

Fuel cell Model

The fuel cell model was developed by experimentally analysing the behaviour of the fuel cell and thus obtaining the polarization curve, from which the direct link between voltage and current is highlighted, as shown in Figure 5.

A 0D and 1D model of the fuel cell has been implemented. They consider the temperature variation of the FC and the surrounding environment (a more detailed thermal model could also consider the temperature variation of the environment surrounding the fuel cell, in the specific case of in which the powertrain is located). In this way it is possible to carry out an ideal control of the fans for the cooling of the FC and therefore to evaluate the thermal profile of the FC and the consumption associated with the fans as the configurations change.

This model does not consider the loss of FC performance due, for example, to possible flooding of the cell or lack of humidity. However, it has been experimentally verified that this phenomenon is almost absent in stationary operating conditions as in the case of a hybrid configuration (FC/SC), therefore this simplified model represents a good compromise in terms of accuracy. For the usefulness of the study it would be a paradox to analyse every single aspect of the different components in detail without any effective return in terms of accuracy [30].

One-converter configuration: Supercapacitors sizing

The sizing of the supercapacitors for the one-converter configuration is divided into the following steps:

- Evaluation of the range within which to vary the voltage of the supercapacitors. In particular this range is determined as the minimum voltage is equal to the minimum voltage sufficient to deliver the desired current to the motor and the maximum voltage is obtained from the assumption that the fuel cell voltage must always be higher than the supercapacitors voltage (since a Buck DC-DC converter is used), so it is considered a value slightly lower than the average voltage that the fuel cell assumes during the race run because by delivering a fixed current, set by the converter, the fuel cell voltage does not vary widely.
- The sizing of the ideal capacitance was carried out through the analysis of the maximum charge variation that the supercapacitors undergo. In particular, the sizing is carried out using the power data related to a power expensive race circuit of the Shell Eco Marathon. The charge variation of the supercapacitors is

evaluated as the difference between the electrical energy consumed by the vehicle and that corresponding to the average power that is constantly supplied by the fuel cell.

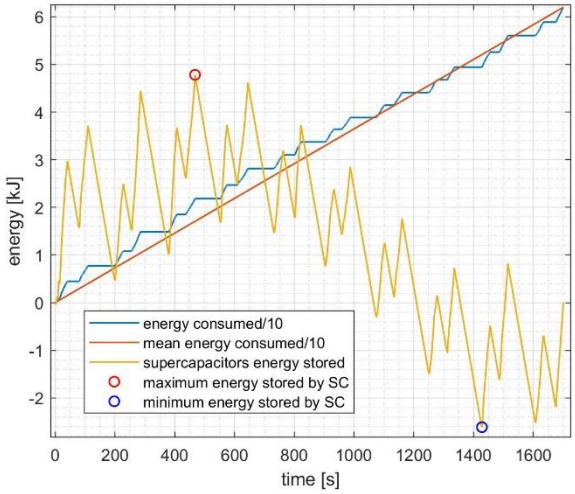

Figure 8. Supercapacitors charge variation

Analyzing the Figure 8 it is possible to identify a minimum and a maximum value of energy stored and, with the difference between these values, it is obtained the variation of minimum energy that has to be compensated by the supercapacitors, then the capacitance is calculated as shown in Eq. (3) and Eq. (4):

$$E_{min} = \frac{1}{2}\, C_{tot} * (V_{C,max}^2 - V_{C,min}^2) \qquad (3)$$

Where: E_{min} is minimum energy that supercapacitors have to compensate, C_{tot} is the total capacitance of supercapacitors, and $V_{C,max}$ and $V_{C,min}$ are the maximum and minimum voltage of supercapacitors.

Knowing these data, with Eq. (4) it is possible to calculate the minimum capacitance to flatten the required current to the fuel cell.

$$C_{tot} = \frac{E_{min}}{\frac{1}{2} * \left(V_{C,max}^2 - V_{C,min}^2\right)} \qquad (4)$$

With this capacitance value the fuel cell can work as desired and cover all power requests during the race.

One-converter configuration: model analysis

To develop a model for this type of configuration it must be known how the DC/DC converter is controlled. In the case of vehicles that runs on a known track, the current supplied by the fuel cell is fixed and is set at the beginning of the path, trying to predict the average power consumed during the run. If the supercapacitors installed have a maximum rated voltage lower than the fuel cell's and lower than the one that could potentially be reached when recharging from the converter, it is necessary to set a maximum voltage limit in order to avoid damaging the supercapacitors. Consequently, the model must consider that if the voltage reaches the maximum value the recharging current must be interrupted.

In the model there are the supercapacitors to which is supplied a charging current, that passing from the converter, comes from the fuel cell and the discharge current that is necessary to supply energy to the motor and auxiliaries. The electric model is formed by two controlled current generators: one that recharges the

capacitors and represents the current coming from the fuel cell, and another that represents the current drawn by the motor and auxiliaries (Figure 9).

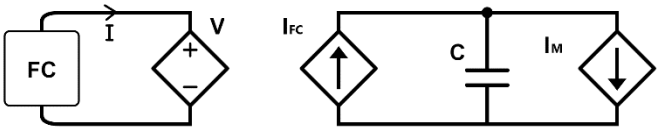

Figure 9. Simplified electric model of one-converter configuration

In this configuration Eq. (5) and Eq. (6) follow:

$$I_{FC} = \frac{P_{FC}}{V_C} * \eta_{converter} \qquad (5)$$

$$I_M = \frac{P_{motor+aux}}{V_C} \qquad (6)$$

Where I_{FC} is the charging current from fuel cell to supercapacitors, V_C the supercapacitors voltage, P_{FC} represents the fuel cell power, $\eta_{converter}$ is the converter efficiency, $I_{M.}$ the motor and auxiliaries current, and $P_{motor+aux}$ is the motor and auxiliaries' power.

The current needed to power the motor and auxiliaries is calculated by dividing the power it absorbs by the voltage of the supercapacitors.

The charging current is calculated considering the power that the fuel cell delivers divided by the supercapacitors voltage and multiplied by the efficiency of the DC-DC converter (Figure 10). The converter efficiency varies according to the voltages and currents of the electrical circuit; however, if during its performance does not vary considerably, the efficiency can be replaced by its mean as a constant. Otherwise the efficiency calculation can be included in the model to obtain more accurate values, as a result the model has a general validity.

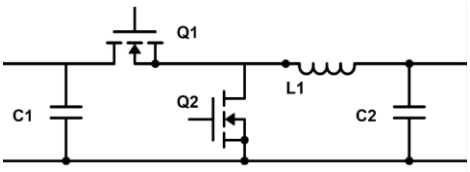

Figure 10. Electric model DC/DC converter

It is necessary to quantify the losses in the various components to calculate the efficiency of the converter. It has to be considered the losses in input and output capacitors (C1 and C2) due to the internal resistance and leakage current, the losses in the inductor series resistance, the losses due to conduction and switching of MOSFETs and losses caused by dead time (MOSFETs do not receive a simultaneous command to avoid that a delay could cause the short circuit of the capacitors, during dead time the current circulates in the parasitic diode of MOSFET Q2 causing losses due to conduction and reverse recovery).

For the efficiency calculation no losses are attributed to the supercapacitors bank because their losses are considered in the model by taking into account the internal resistance (Figure 11 and Eq. (7)).

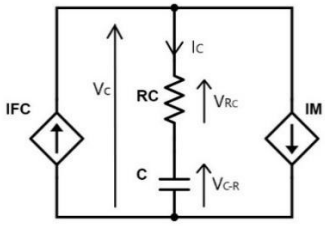

Figure 11. Simplified electric model of the powertrain

$$\begin{cases} I_C = I_{FC} - I_M = C * \frac{dV_{C-R}}{dt} \\ V_C = R_C * I_C + V_{C-R} \end{cases} \qquad (7)$$

Where: I_C represents the supercapacitors current, R_C is the internal resistance, and V_{C-R} their voltage (without resistance).

The model implemented in the Simulink environment is illustrated in Figure 12.

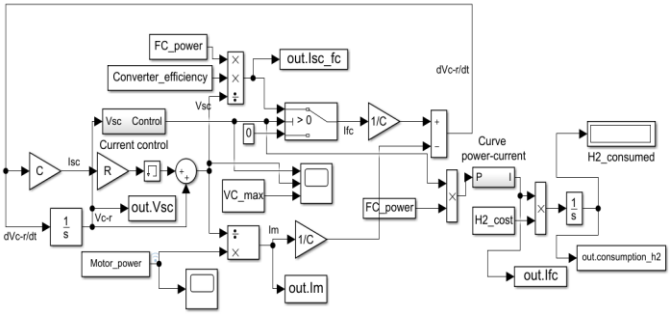

Figure 12. One-converter configuration Simulink model

Passive charging configuration: model analysis

The starting point for the development of a passive charging model (direct parallel configuration) is the electrical scheme as shown in Figure 13, and the relative equations in the system in Eq. (8).

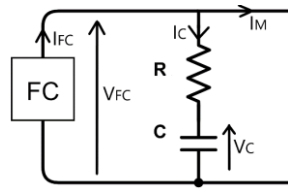

Figure 13. Electrical scheme passive charging configuration

$$\begin{cases} V_{FC} = V_C + R\, I_C \\ I_{FC} = f(V_{FC}) = a\, {V_{FC}}^3 + b\, {V_{FC}}^2 + c\, V_{FC} + d \\ I_{FC} = I_C + I_M \\ I_C = C\,\dfrac{\partial V_C}{\partial t} \\ P = V_{FC}\, I_M \end{cases} \quad (8)$$

Where a,b,c,d are polynomial coefficients used to estimate the polarization curve.

From the system of Eq. 8 with substitutions, it can be obtained the differential equations in Eq. (9).

$$\begin{cases} \dfrac{\partial V_C}{\partial t} = \dfrac{f(V_{FC})}{C} + \dfrac{R}{V_C}\dfrac{\partial V_C}{\partial t} f(V_{FC}) - \dfrac{RC}{V_C}\left(\dfrac{\partial V_C}{\partial t}\right)^2 - \dfrac{P}{C\, V_C} \\ V_{FC} = V_C + RI_{SC} = V_C + RC\dfrac{\partial V_C}{\partial t} \end{cases} \quad (9)$$

The Eq. (9) was developed in Simulink (Figure 14). The model receives as input data the polarization curve, the capacitance, the internal resistance of the supercapacitors and the power required by the motor and auxiliaries; and provides the output voltage and current trends of the fuel cell, which allows the calculation of hydrogen consumption.

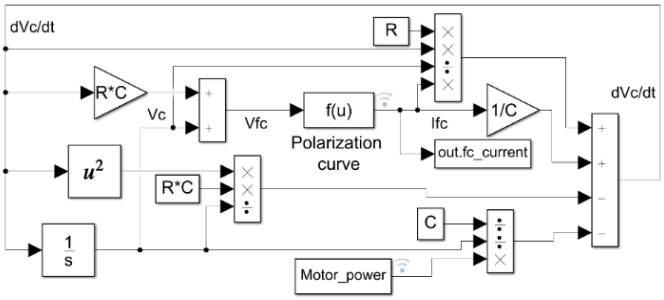

Figure 14. Simulink passive charging model

In particular, the consumption of hydrogen is tightly related to the current supplied and purges as shown in Eq.(10):

$$H_2^{flow} = (H_2 molar\ vol.) * \frac{I}{2 * (F)} * nc + H_{2\,purged}^{flow} \quad (10)$$

Where: H_2^{flow} is the hydrogen flow consumption, H_2 molar vol is hydrogen molar volume, F the Faraday constant, *nc* the number of cells of fuel cell, $H_{2purged}^{flow}$ represents the hydrogen flow lost during purges.

The polarization curve block, which can be seen in Figure 14, implements the polynomial equation (shown in the 2nd line of Eq. (8)) that having as input the fuel cell voltage returns the fuel cell current supplied.

Passive charging configuration: supercapacitors sizing

In order to understand the effect of supercapacitors capacitance on consumption, a Simulink model has been developed neglecting their internal resistance (Figure 15). The Eq. (11) implemented is:

$$\frac{\partial V_{FC}}{\partial t} = \frac{1}{C}\,(I_{FC} - I_M) \qquad (11)$$

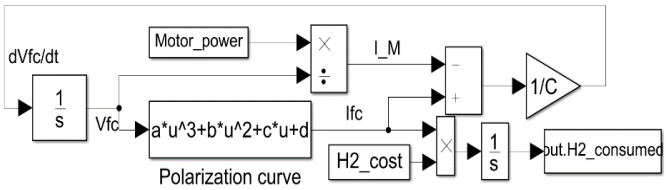

Figure 15. Passive charging Simulink model (no internal resistance)

The development of a MATLAB program allows the calculation of hydrogen consumption as the capacitance varies within a range of interest. In order to have significant values, the final voltage needs to be higher than the initial one due to competition's regulation, otherwise the supercapacitors would provide energy that would not be considered in consumptions. Through a "while cycle" the simulation is repeated using an algorithm until the final voltage is at least as close to the initial one. Another technique to make a true comparison between the different simulation results is to use for every simulation the same starting voltage and to sum to the final consumption an additive quantity.

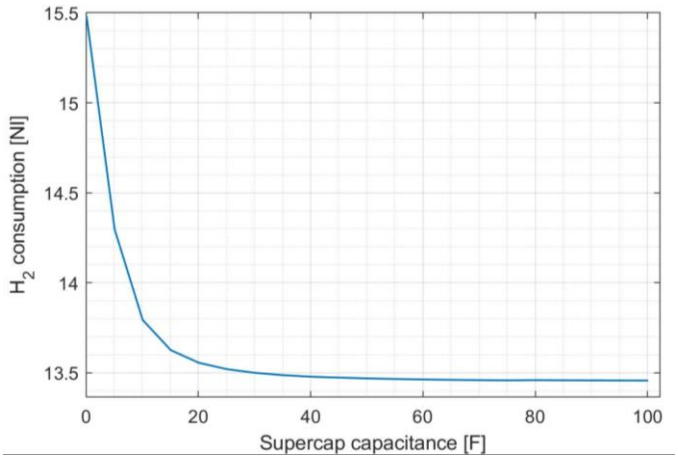

Figure 16. Hydrogen consumption as a function of capacitance

This additive value can be calculated considering the quantity of hydrogen that would be consumed by the fuel cell in order to bring the supercapacitors voltage to the starting value. Than thanks to a "for cycle" several simulations are performed for different capacitance, so it is possible to draw a capacitance-consumption graph (Figure 16). Near-zero Farad is the capacitance corresponding to the use of the configuration with only fuel cell and, as the result of these simulations, this configuration is the less efficient because it consumes a larger amount of hydrogen.

As the result of these simulations, the graph in Figure 16 shows how the consumption decreases as the capacitance increases, tending to a horizontal asymptote. From the graph can be chosen a capacitance value sufficiently high that the consumption can be assumed as the asymptote value. The identified capacitance value will be the minimum value used for the following step in which the focus is on current fluctuations as the capacitance changes, which allows to make other evaluations on the behavior of the fuel cell.

To take into consideration how the capacitance can affect the behavior of the fuel cell in terms of current fluctuations, the trends shown in Figure 17 of the current supplied by the fuel cell shall be observed, corresponding to a race attempt of the vehicle.

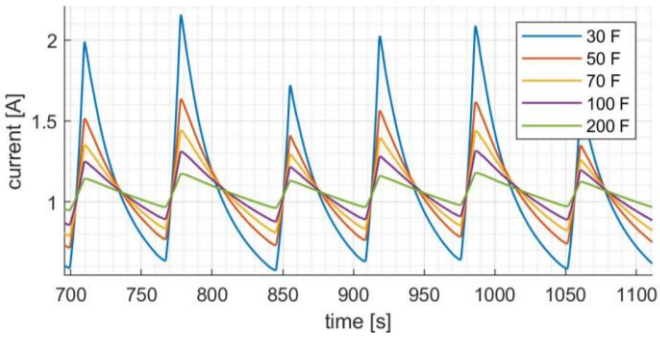

Figure 17. Current profile as a function of capacitance

As expected, the model shows how the amplitude of the current oscillations decreases as the capacitance of the supercapacitors increases. The range of oscillations of the current affects the behavior of the fuel cell, the use of a high capacitance allows to stabilize the current and avoid peaks. As explained in the theoretical analysis, limiting the peaks and working in a steady state avoids the problems related to performance losses and therefore also limits the use of short-circuit and purge techniques which involve an additional consumption of hydrogen.

Although they are already with the capacitance identified in the previous point reduced much compared to the configuration without supercapacitors, the use of a higher capacitance allows to obtain better performance.

To quantify how much the current fluctuation affects the behavior of the fuel cell, it is necessary to conduct experimental tests in the laboratory to analyze a specific fuel cell, because each fuel cell responds differently to it. These steps can be followed:

- Starting from the passive charging model and the power data of a race circuit, the current that the fuel cell would deliver during the race is calculated and this is done for various capacitance values in a range of interest;
- The experimental tests are conducted with the currents obtained in the previous step, for each experimental test are measured the hydrogen consumption ($V_{H2_{test}}$) and the average power delivered by the fuel cell (P_{test});
- The consumptions obtained for each test are rationalized to the average power reference (Eq. (12)). The average power reference ($P_{reference}$) corresponds to the average power requested by the real race circuit.

$$V_{H2_{rationalized}} = V_{H2_{test}} * \frac{P_{reference}}{P_{test}} \quad (12)$$

- then it is composed a graph that shows the consumption of hydrogen ($V_{H2_{rationalized}}$) as a function of capacitance.

It is possible to bring the hydrogen consumption back to the reference power because if the average power of the test does not differ much from the average reference power, it can be considered a linear variation of consumptions.

This method allows to obtain an information about the performance of specific fuel cell that corresponds to different current fluctuation intensities. Therefore, it is possible assess if higher capacitances provide real advantages, or if the capacitance originally obtained the fuel cell maintains good humidification of the membrane and high performance, without purges and short circuits described before.

In addition, the influence of the choice of supercapacitors on vehicle dynamics must also be taken into account in order to make a complete assessment, in particular the influence on the weight of the vehicle.

Another parameter to be taken into account is the thermal behavior of the FC as the chosen supercapacitors configuration changes. The graph in Figure 18 shows how the use of a higher capacity leads to an advantage in thermal terms.

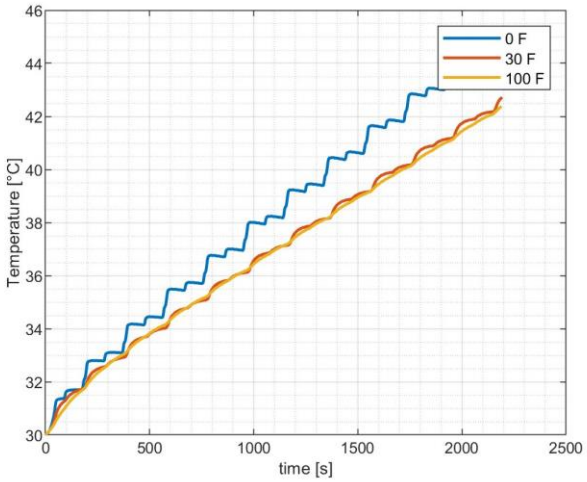

Figure 18. Temperature trends as the capacitance of supercapacitors changes

The Figure 18 shows that increasing the capacitance also has advantages from the point of view of temperature control, and consequently there are advantages in terms of the fuel cell's efficiency and the reduction of energy consumption associated with the auxiliaries used to control the temperature (in this case study the consumption of the fans is reduced). The temperature trends were obtained by using the 0D thermal model briefly presented in section “ Fuel cell Model ”.

Dynamic Model

In order to compare the different powertrain configurations proposed, it was necessary to develop a model of the dynamics that allows the energy required by the powertrain to be evaluated as the race track changes.

The equations needed to develop vehicle dynamics in Simulink, have been obtained from a free body diagram (Figure 19).

It has been decided to study the dynamics with a 1 degree of freedom model, the track is a straight line with ups and downs, but the effect of curves is neglected. With this simplification the weight on each of the front wheels is the same, therefore in the calculations can consider having a single front wheel with double inertia and rolling resistance [31].

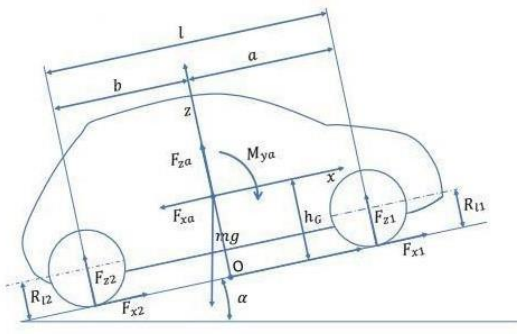

Figure 19. Free body diagram

The equation obtained is:

$$m_a \frac{\partial V}{\partial t} = \eta_t \frac{M_m}{R\tau_p} - \left(\frac{1}{2}\rho V^2 C_x S + mgsin\alpha\right) - (f_1 F_{z1} + f_2 F_{z2}) \quad (13)$$

Where F_{z1}, F_{z2} and R are respectively equal to:

$$F_{z1} = \frac{mg(bcos\alpha - h_G sin\alpha) - bF_{za} - h_G F_{xa} + Mya - mh_G \dot{V}}{l} \quad (14)$$

$$F_{z2} = \frac{mg(acos\alpha + h_G sin\alpha) - aF_{za} + h_G F_{xa} - Mya - mh_G \dot{V}}{l} \quad (15)$$

$$R = \frac{R_0}{1 + \delta} \quad (16)$$

The mass m_a is the equivalent mass that takes into account linear inertia (vehicle mass m) and rotational inertia (of the rotating masses) and can be calculated as:

$$m_a = m + \frac{J_r}{R^2} + \frac{J_m}{R^2} * \left(\tau_p \tau_g\right)^2 \quad (17)$$

Where J_r and J_m are respectively the moment of inertia of the wheel and motor+sprocket, V is the vehicle speed, M_m is the torque delivered by the electric motor, R_0 is the geometric wheel radius and R is the corrected value taking into account the longitudinal slip δ.

τ_p is the transmission ratio between the engine and the wheel, while τ_g is the transmission ratio of the differential (in the case under consideration, since it is not present, is equal to 1).

F_{xa} and F_{za} consist of vertical and frontal frictional forces. The first force can be neglected due to the low speeds reached (<40 km/h) and the streamlined shape of the vehicle, while the second is calculated as:

$$F_{z2} = \frac{1}{2}\rho V_{w2v}^2 S C_x \qquad (18)$$

Where V_{w2v} is the speed of the vehicle with respect to the air, S is the frontal area, C_x is the coefficient of aerodynamic resistance and ρ is the air density. The rolling resistance coefficients at the wheels are considered equal: $f_1 = f_2 = f$.

The value of f depends on the speed of the vehicle, but at low speeds it can be considered constant, as in the case under consideration.

a, b and h_G are values needed to find the position of the center of gravity (as shown in Figure 19).

Substituting the equations (14) and (15) in (13) is obtained:

$$m_a \frac{\partial V}{\partial t} = \frac{\eta_t}{R\tau_p} M_m - \frac{1}{2}\rho V^2 C_x S - f\, m\, g\, cos - m\, g\, sin\alpha \qquad (19)$$

By implementing this equation in Simulink, it is possible to obtain the torque that must be supplied to the vehicle in order to maintain a given reference speed.

A forward approach [32–34] was chosen for modelling, which can be summarized in the diagram presented in the Figure 20.

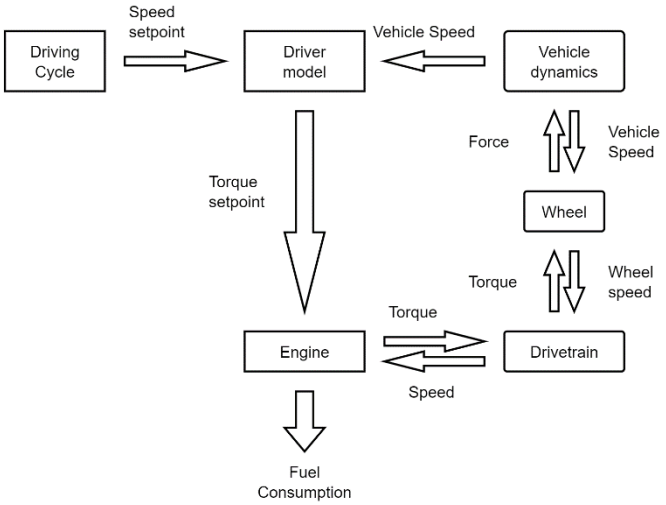

Figure 20. Forward modeling flow chart

The Figure 20 shows the main steps:

- Driving cycle speed is compared with the actual vehicle speed;
- Driver model generates braking and throttle commands;
- Commands are sent to the supervisor block responsible to generate the actuators set points.

In addition, experimental data obtained on the racetrack can be used to evaluate the different configurations, which can be fed into the powertrain model.

Then, it is known the torque that must be supplied to the wheel and the speed of the vehicle, so since the transmission ratio and efficiency are known, it is possible to obtain the torque that must be supplied by the motor and its angular speed as in Eq. (20) and (21).

$$\omega_m = \omega_w * (\tau_P * \tau_g) \quad (20)$$

$$T_m = \frac{T_w}{\tau_P * \tau_g} \quad (21)$$

Where ω_m and ω_w are respectively the angular speed of the motor and wheel and T_m and T_w are respectively the torque of the motor and wheel.

These values are used in the electric motor model to estimate the voltage and current to be supplied to this component. The motor used on the IDRAkronos vehicle is a brushed DC electric motor, so it can be modelled synthetically with its typical Eq. (22) and (23).

$$E_a = k_E * \omega_m \quad (22)$$

$$T_m = k_T * I_a \quad (23)$$

Where k_E and k_T are respectively the motor speed constant and motor torque constant, E_a is the inducted voltage and I_a is the armature current.

The Eq. (22) and (23) allow to correlate electrical and mechanical quantities, but to obtain the armature voltage at the motor terminals, the voltage drop across the inductance of the armature windings and their resistance must also be taken into account. As a result of the Kirchhoff current law the equation Eq. (24) can then be written.

$$V_a = E_a + R_a * I_a + L_a * \frac{\partial I_a}{\partial t} \quad (24)$$

Where V_a is the armature voltage, R_a is the armature resistance and L_a is the armature inductance. In this way the voltage and current of the motor are known, but in order to supply it from the supercapacitors, it is necessary to make the connection between them using a power converter. In the case in consideration, a Buck DC/DC converter made from an inverter leg was used. At a given supercapacitor voltage, in order to determine the current that must be supplied by the supercapacitors to power the motor the converter must be modelled. The converter can be modelled in a simplified way by considering the energy conservation and its efficiency as shown in the Eq. (25) and (26). However, the efficiency of the converter is not constant but varies with the input and output voltages and currents. It is therefore necessary to quantify the various losses such as conduction and switching losses [35].

$$P_{in} * \eta_{conv} = P_{out} \quad (25)$$

$$V_{in} * I_{in} * \eta_{conv} = V_{out} * I_{out} \quad (26)$$

Where P_{in} and P_{out} are respectively the input and output power of the converter, η_{conv} is the efficiency of the converter, V_{in} and V_{out} are respectively the input and output voltage of the converter while $I_{in}\ and\ I_{out}$ are respectively the input and output current of the converter.

Results

The models and the sizing methods shown above have general validity, but in order to conduct a clearer comparison and give an idea of the capacitance and consumption values that could be obtained from the sizing methods seen and the proposed models, the results related to the case-study of IDRAkronos vehicle are provided.

In particular, for the evaluation of the results, experimental data obtained on a racing circuit was used as input to the powertrain model.

The Figure 21 shows the power data given as input to the different simulations:

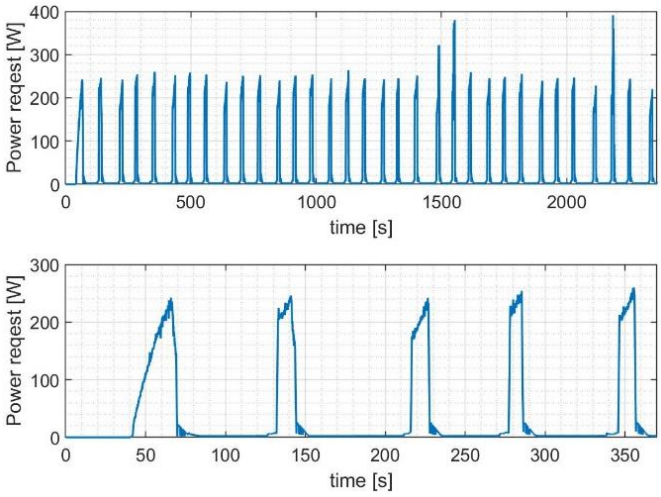

Figure 21. Experimental obtained power request used in simulations

One-converter configuration: Supercapacitors sizing

The data used for the polarization curve refers to the PEMFC HORIZON H500 with 44 cells, and the power data is from the race circuit most energy demanding. This information was already reported in Figure 8, where the graph shows, during the run, the difference between the integral of the power required by the motor and the integral of the average power. By making the difference between the maximum and minimum values, it was obtained the amount of energy that must be compensated by the supercapacitors, it corresponds to 7394 J. As minimum voltage was used the nominal voltage of the 24V motor (since the motor is powered by a Buck converter) and 32V as maximum which is a voltage slightly lower than the one assumed by the fuel cell, when it delivers the average power of the race considered. Then, a supercapacitors capacitance of 33F was calculated and it was realized with 12 EATON XT 400F supercapacitors in series. With this capacitance value it is possible that the fuel cell works as desired and to cover all power requests.

Passive charging configuration: supercapacitor sizing

The sizing of the supercapacitor in the case-study was carried out using the 44-cell PEMFC Horizon H500 and considering the power required by the Shell Eco Marathon race circuit.

It can be deduced from the virtual model that when reaching capacitances around 40 F the consumption tends to the asymptote. However, this assumption deviates slightly from the real behavior. The increase in capacitance also presents an advantage in terms of stabilization of the current. This advantage does not emerge from the model, but through the experimental tests it was clear that for the PEMFC HORIZON H500 the best in terms of performance is obtained for a capacitance value around 100 F. Furthermore, during the sizing phase, the supercapacitors' efficiency and weight must be considered.

The tradeoff between the different parameter points to the lithium ion capacitors as the best choice. Therefore, the ULTIMO 1100 F supercapacitors were chosen. Connecting 11 of them in series to form a bank of capacitors, it reaches a capacitance of 100 F and a maximum rated voltage of 41.8 V, their weight is contained to only 1.57 kg.

Comparison and validation of the models with the experimental results

The results obtained with the passive charging model and the DC/DC converter model were validated through the experimental tests carried out in the laboratory and the track tests carried out during the Shell Eco Marathon 2019 in the Netherlands and in the UK.

Table 2. Consumption results for different configuration

Configuration	Model [km/Nm^3]	Lab. Test	On Track
FC	1035	940	1023
DC/DC	1075	1060	1058
Passive	1146	1110	-
Passive	1160	-	-

Table 2 shows that for the configuration without the use of supercapacitors the result in terms of km//Nm^3 from the model is about 9% higher than that obtained through experimental tests in the laboratory. This emerges because the model does not consider the dynamics of the fuel cell but approximates its behaviour using an average polarization curve. In fact, during the simulation it was noted that due to the variable operation of the fuel cell there was a deterioration in performance.

While the result obtained on the track of 1023 km/Nm^3 was obtained on a different circuit than the one used as a reference for the models and simulations in the laboratory. This race circuit required an overall average power 11% lower than the reference circuit, then the consumption value obtained on the track can be equated in quantitative terms to that obtained in the laboratory.

Figure 22 shows that during the first phases of the track, the voltage trend of the fuel cell during the experiment is equivalent to the one simulated, while subsequently efficiency diminishes leading to a higher H_2 consumption. Specifically, it is possible notice as the voltage decreases the most during the acceleration phases.

Figure 23 shows that the FC operating in non-hybrid configuration must deliver the whole power required instant by instant, making the load and power curves coincident. This operation is particularly disadvantageous in situations in which the load is highly variable.

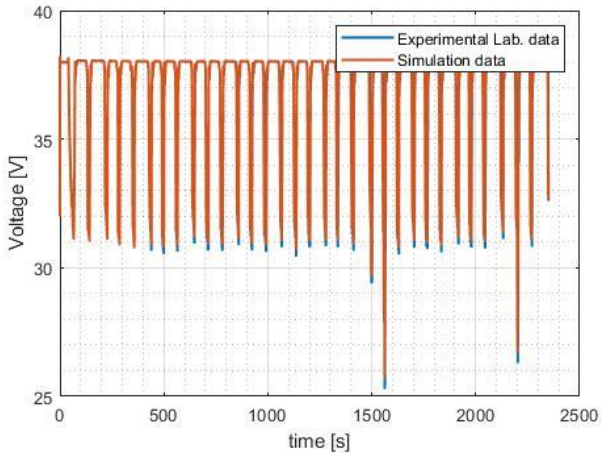

Figure 22. Fuel cell configuration: simulation data vs experimental data

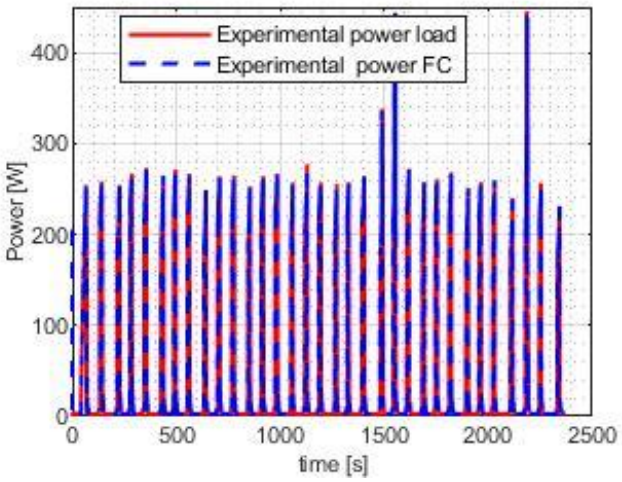

Figure 23. Fuel cell configuration: power load vs power FC

Table 2 shows the model's consumption for the DC/DC configuration is consistent and equivalent with the results obtained through the tests in the laboratory and on the track. Figure 24 highlights how, using the DC/DC converter and supercapacitors, it is possible to have a steady state operation of the fuel cell and therefore to improve performance compared to the configuration without supercapacitors.

Furthermore, Figure 24 supports fact that the supercapacitors can manage the load peaks required by the motor.

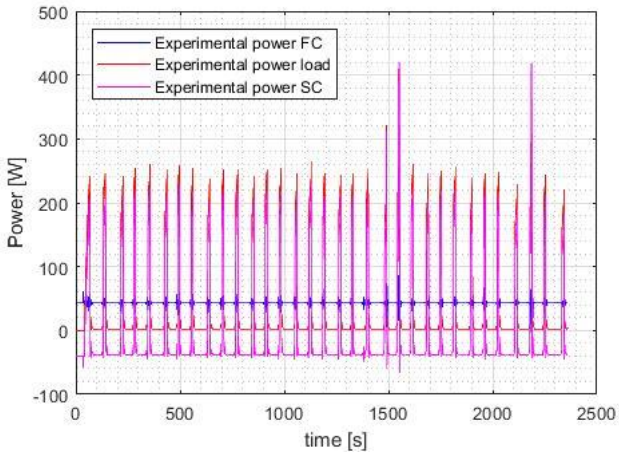

Figure 24. DC/DC configuration: power load vs power FC vs power SC

Figure 25 illustrates the experimental data obtained on the track, which presents higher oscillation than the model's result. These oscillations occur mainly during the acceleration phases. The results in terms of average currents differ by about 1.5% and therefore the model is equivalent to the experimental results obtained on the track and in the laboratory.

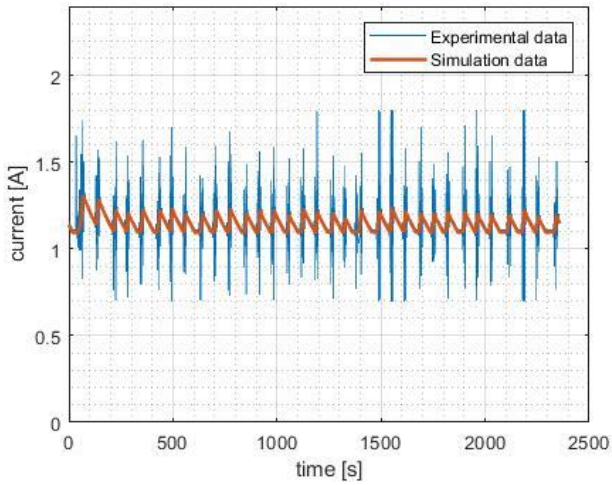

Figure 25. DC/DC configuration: simulation data vs experimental data

As presented by Table 2 for the passive configuration, it was possible to validate the model through experimental simulations in the laboratory using a bank of supercapacitors with a capacitance of 33 F (EATON XT). The consumption result is higher than that obtained from the model due to a worsening of the performance of the fuel cell related to the necessity of high capacitance for ideal operation. Since the experimental average voltage is lower, in order to supply the same energy, amount the mean current is higher.

Therefore, as presented in Figure 26, the voltage for experimental data has larger oscillations and consequently the current has larger fluctuations.

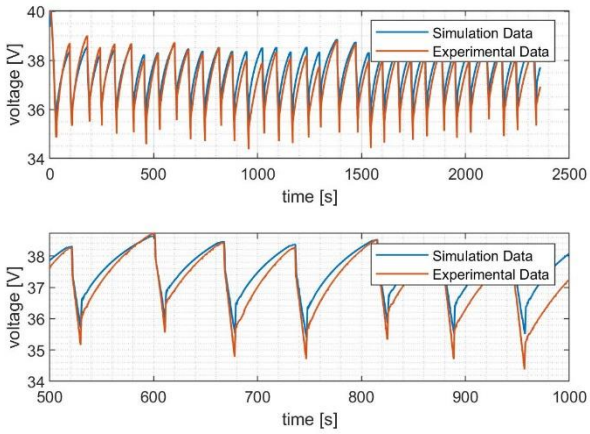

Figure 26. Passive charging: simulation data vs experimental data

The voltage fluctuations in Figure 26 correspond to the variable power demand that at irregular time intervals discharges the supercapacitors while they are constantly recharged by the fuel cell. The discontinuities in the peaks are due to the effect of the supercapacitor's resistance.

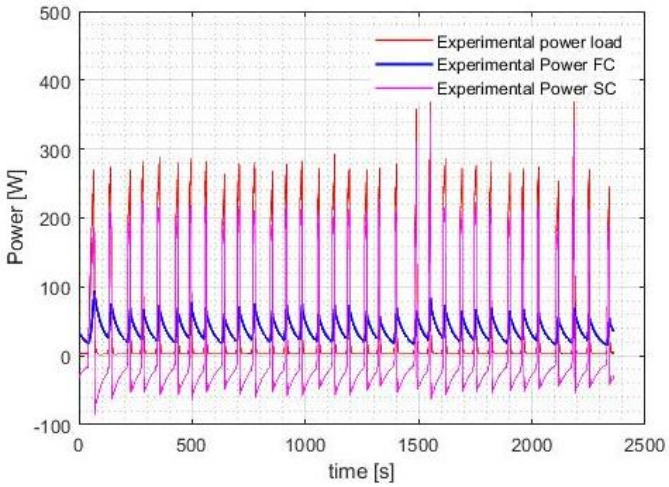

Figure 27. Passive charging configuration: Load, FC and SC power

Experimental voltage trend in the first phase is higher than the one of the simulations. During the race run the performance of the fuel cell, in the absence of short circuits and purges, worsen over time and approaches to the polarization curve. At the end the experimental voltages of the fuel cell are lower than those of the simulation. This is due to the FCs performances that initially are better than the polarization curve provided to the model[3].

Figure 27 shows the capacitance of the supercapacitors acts as a buffer towards the fuel cell. In this way it is possible to notice how the fuel cell provides the base load while the supercapacitors ensure the compensation of the peaks required by the motor.

3 The polarization curve supplied to the model is an average curve, which considers the possible worsening of the performance of the fuel cell mainly due to a non-uniform humidification of the membrane.

The power curve of the supercapacitors reaches negative values during the coast down phase which therefore represents a charging phase, being the power required by the load lower than the average power supplied by the Fuel cell.

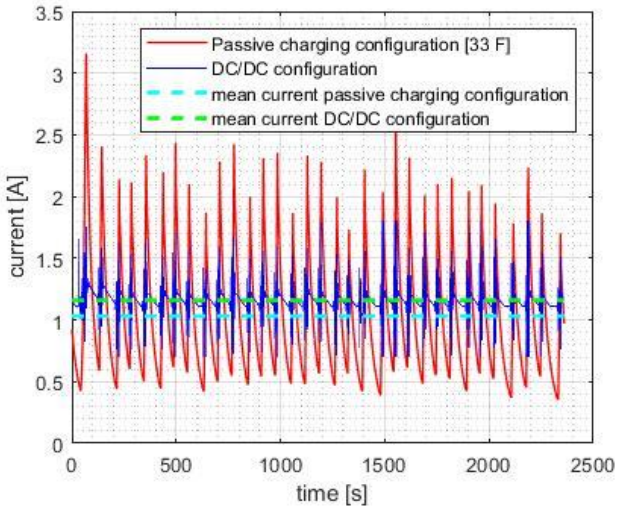

Figure 28 - Comparison experimental data: passive charging vs DC/DC configuration

By analysing Figure 28, it can be seen how the DC/DC configuration is able to guarantee lower oscillations compared to the passive charging configuration but the average value of the current is higher than that of passive charging and therefore the consumption of hydrogen will be higher.

Conclusions

This paper presents different possible configurations for the powertrain of an FCEV and it analyses in detail, using a simulation model, the sizing criteria for supercapacitors and the optimization processes. The models were validated through experimental tests in the laboratory and on the track.

During these tests it was noted how the use of supercapacitors represents a suitable solution for all the applications where a variable load is required. Specifically, the configuration with the DC/DC converter guarantees greater control while the "passive charging" configuration guarantees greater efficiency.

It was also analysed how the passive charging configuration requires an oversizing of the supercapacitor capacitance in order to maximize efficiency and reduce current oscillations .This oversizing consequently leads to an increase in weight, it will therefore be necessary to trade-off between the increase in efficiency and the greater losses due to vehicle dynamics.

These models are useful in order to quantify the hydrogen consumption for the different configurations. It is possible to study which configuration is the more suitable for a particular application, and so they can be useful in the design phases of the powertrain of a FCEV. Another possible application concerns road vehicles. By including this model into an integrated model of the vehicle (which then considers the dynamics of the vehicle, the motor and its driver) it allows for calculating the consumption of a specific route. This could allow, for example, for self-driving vehicles to choose the route with the lowest consumption. Therefore, with a view to sustainable development and reduction of emissions, the FCEVs represent an excellent solution.

Future developments on this paper will focus mainly on the development of tests on the track regarding the “passive charging configuration” and the in-depth tests performed with the bank of supercapacitors with higher capacitance.

References

1. International Energy Agency, “Total CO2 emissions by sector in 2018,” https://www.iea.org/data-and-statistics?country=WORLD&fuel=CO2%20emissions&indicator=CO2BySector, Oct. 2020.

2. International Energy Agency, “Total final consumption by sector in 2018,” https://www.iea.org/data-and-statistics?country=WORLD&fuel=Energy%20consumption&indicator=TFCShareBySector, Oct. 2020.

3. Ball, M. and Weeda, M., “The hydrogen economy – Vision or reality?,” *Int. J. Hydrog. Energy* 40(25):7903–7919, 2015, doi:10.1016/j.ijhydene.2015.04.032.

4. Carello, M., Airale, A.G., and Messana, A., “IDRApegasus: a carbon fiber monocoque vehicle prototype,” *Mater. Werkst.* 45(5), 2014, doi:10.1002/mawe.201400238.

5. Messana, A., Sisca, L., Ferraris, A., Airale, A.G., Carvalho Pinheiro, H. de, Sanfilippo, P., and Carello, M., “From Design to Manufacture of a Carbon Fiber Monocoque for a Three-Wheeler Vehicle Prototype,” *Materials* 12(3):332, 2019, doi:10.3390/ma12030332.

6. De Cupis, D., Carvalho Pinheiro, H. de, Ferraris, A., Airale, A.G., and Carello, M., “Active Aerodynamics Design Methodology for Vehicle Dynamics Enhancement,” in: Niola, V. and Gasparetto, A., eds., *Advances in Italian Mechanism Science*, Springer International Publishing, Cham, ISBN 978-3-030-55807-9: 777–785, 2021, doi:10.1007/978-3-030-55807-9_86.

7. Carello, M., Andrea, S., Airale, A.G., and Ferraris, A., “Design the City Vehicle XAM using CFD Analysis,” *SAE 2015 World Congress & Exhibition*, SAE Technical Paper 2015-01-1533, 2015, doi:10.4271/2015-01-1533.

8. Ferraris, A., Airale, A.G., Berti Polato, D., Messana, A., Xu, S., Massai, P., and Carello, M., “City Car Drag Reduction by Means of Shape Optimization and Add-On Devices,” in: Uhl, T., ed., *Advances in Mechanism and Machine Science*, Springer International Publishing, ISBN 978-3-030-20131-9: 3721–3730, 2019, doi:10.1007/978-3-030-20131-9_367.

9. Carello, M., Ferraris, A., Airale, A., and Fuentes, F., “City Vehicle XAM 2.0: Design and Optimization of its Plug-In E-REV Powertrain,” SAE Technical Paper 2014-01-1822, 2014, doi:10.4271/2014-01-1822.

10. Carello, M. and Messana, A., “IDRA pegasus: a fuel-cell prototype for 3000 km/L,” *Comput.-Aided Des. Appl.* 12(sup1):56–66, 2015, doi:10.1080/16864360.2015.1077076.

11. Brusaglino, G., Buja, G., Carello, M., Carlucci, A.P., Onder, C.H., and Razzetti, M., “New technologies demonstrated at Formula Electric and Hybrid Italy 2008,” *World Electr. Veh. J.* 3(1):160–171, 2009, doi:10.3390/wevj3010160.

12. Filippo, N., Carello, M., D’Auria, M., and Marcello, A., “Optimization of IDRApegasus: Fuel Cell Hydrogen Vehicle,” SAE Technical Paper 2013-01-0964, 2013, doi:10.4271/2013-01-0964.

13. Dadam, S.R., Jentz, R., lenzen, T., and Meissner, H., “Diagnostic Evaluation of Exhaust Gas Recirculation (EGR) System on Gasoline Electric Hybrid Vehicle,” 2020-01–0902, 2020, doi:10.4271/2020-01-0902.

14. Sofo, A., “I biocombustibili: vantaggi, problematiche e reali possibilità di diffusione”. Online document available at: http://oldwww.unibas.it/utenti/sofo/Sofo_biodiesel.pdf, Oct. 2020.

15. Larminie, J. and Dicks, A., “Fuel Cell Systems Explained,” John Wiley and Sons, Inc., New York, ISBN 978-0-470-84857-9, 2000.

16. Thounthong, P., Rael, S., and Davat, B., “Utilizing fuel cell and supercapacitors for automotive hybrid electrical system,” *Twentieth Annual IEEE Applied Power Electronics Conference and Exposition, 2005. APEC 2005.*, 90-96 Vol. 1, 2005, doi:10.1109/APEC.2005.1452894.

17. Atwood, P., Gurski, S., Nelson, D.J., Wipke, K.B., and Markel, T., “Degree of Hybridization Modeling of a Hydrogen Fuel Cell PNGV-Class Vehicle,” SAE Technical Paper 2002-01–1945, SAE International, Warrendale, PA, 2002, doi:10.4271/2002-01-1945.

18. Huang, M., Wen, P., Zhang, Z., Wang, B., Mao, W., Deng, J., and Ni, H., “Research on hybrid ratio of fuel cell hybrid vehicle based on ADVISOR,” *Int. J. Hydrog. Energy* 41(36):16282–16286, 2016, doi:10.1016/j.ijhydene.2016.05.130.

19. KoteswaraRao.K, V. and Srinivasulu, G.N., “Modeling, downsizing, and performance comparison of a fuel cell hybrid mid-size car with FCEV for urban and hill road driving cycles,” *Int. J. Green Energy* 16(2):115–124, 2019, doi:10.1080/15435075.2018.1549996.

20. Nassif, G.G. and Almeida, S.C.A. de, “Impact of powertrain hybridization on the performance and costs of a fuel cell electric vehicle,” *Int. J. Hydrog. Energy* 45(41):21722–21737, 2020, doi:10.1016/j.ijhydene.2020.05.138.

21. Becherif, M., Ayad, M.Y., and Miraoui, A., “Modeling and Passivity-Based Control of Hybrid Sources: Fuel Cell and Supercapacitors,” *Conference Record of the 2006 IEEE Industry Applications Conference Forty-First IAS Annual Meeting*, 1134–1139, 2006, doi:10.1109/IAS.2006.256675.

22. Azib, T., Bethoux, O., Remy, G., Marchand, C., and Berthelot, E., “An Innovative Control Strategy of a Single Converter for Hybrid Fuel Cell/Supercapacitor Power Source,” *IEEE Trans. Ind. Electron.* 57(12):4024–4031, 2010, doi:10.1109/TIE.2010.2044123.

23. Garcia Arregui, M., “Theoretical study of a power generation unit based on the hybridization of a fuel cell stack and ultra capacitors,” Ph.D. dissertation, Institut National Polytechnique de Toulouse, Toulouse, France, Dec. 4, 2007.

24. Rajashekara, K., “Propulsion System Strategies for Fuel Cell Vehicles,” 2000-01–0369, 2000, doi:10.4271/2000-01-0369.

25. Dépature, C., Macías, A., Jácome, A., Boulon, L., Solano, J., and Trovão, J.P., “Fuel cell/supercapacitor passive configuration sizing approach for vehicular applications,” *Int. J. Hydrog. Energy* 45(50):26501–26512, 2020, doi:10.1016/j.ijhydene.2020.05.040.

26. Carello, M., Vita, A.D., and Ferraris, A., “Method for Increasing the Humidity in Polymer Electrolyte Membrane Fuel Cell,” *Fuel Cells* 16(2):157–164, 2016, doi:10.1002/fuce.201500110.

27. Ferraris, A., Messana, A., Airale, A.G., Sisca, L., Carvalho Pinheiro, H. de, Zevola, F., and Carello, M., “Nafion® Tubing Humidification System for Polymer Electrolyte Membrane Fuel Cells,” *Energies* 12(9):1773, 2019, doi:10.3390/en12091773.

28. Dhaliwal, A., Nagaraj, S.C., and Ali, S., “Hardware-in-the-Loop Simulation for Hybrid Electric Vehicles – An Overview, Lessons Learned and Solutions Implemented,” 2009-01–0735, 2009, doi:10.4271/2009-01-0735.

29. Kandavelu, S., Velagapudi, A.K., Nese, R., and Thimmalapura, S., “A Cost Effective System Test-Bed using Model Based Approach,” 2016-01–0048, 2016, doi:10.4271/2016-01-0048.

30. Zhu, D., Pritchard, E.G.D., and Silverberg, L.M., “A New System Development Framework Driven by a Model-Based Testing Approach Bridged by Information Flow,” *IEEE Syst. J.* 12(3):2917–2924, 2018, doi:10.1109/JSYST.2016.2631142.

31. Genta, G. and Morello, L., “The Automotive Chassis: Volume 1-2,” Springer Science & Business Media, ISBN 978-1-4020-8676-2, 2008.

32. Zahraei, M.S., Jazayeri, S.A., Shahbakhti, M., and Sharifirad, M., “Look-forward longitudinal dynamic modelling for a series-parallel hybrid electric vehicle,” *Int. J. Electr. Hybrid Veh.* 1(4):342–363, 2008, doi:10.1504/IJEHV.2008.022261.

33. Chacko, R.V., Sreedevi, M.L., and Mineeshma, G.R., “Electric vehicle power train simulation in forward modelling approach to enable real-time simulation and HIL controller prototyping,” *2014 IEEE International Conference on Power Electronics, Drives and Energy Systems (PEDES)*, 1–6, 2014, doi:10.1109/PEDES.2014.7042039.

34. Hofman, T., Leeuwen, D. van, and Steinbuch, M., “Analysis of modelling and simulation methodologies for vehicular propulsion systems,” *Int. J. Powertrains* 1(2):117–136, 2011, doi:10.1504/IJPT.2011.042763.

35. Carvalho Pinheiro, H. de, Castro dos Santos, P.G., Sisca, L., Scavuzzo, S., Ferraris, A., Airale, A.G., and Carello, M., “Dynamic Performance Comparison Between In-Wheel and On-Board Motor Battery Electric Vehicles,” American Society of Mechanical Engineers Digital Collection, 2020, doi:10.1115/DETC2020-22306.

Contact Information

Massimiliana Carello
massimiliana.carello@polito.it

Henrique de Carvalho Pinheiro
henrique.decarvalho@polito.it

Leonardo Longega
leonardolongega1234@gmail.com

Luca Di Napoli
lucadinapoli2@gmail.com

Definitions/Abbreviations

FCEV	Fuel Cell Electric Vehicle
PEM	Proton-exchange membrane
ICE	Internal Combustion Engine
MHEV	Mild Hybrid Electric Vehicle
HEV	Hybrid Electric Vehicle
PHEV	Plug-in Hybrid Electric Vehicle
BEV	Battery Electric Vehicle
FC	Fuel Cell

SC	Supercapacitor
DOH	Degree of hybridization
EDLC	Electric double-layer capacitors
LIC	Lithium-ion supercapacitor
MOSFET	Metal Oxide Semiconductor Field Effect Transistor